53±18 mg/dl だった。BMI25 以上の肥満者は 30%, 、高血圧の合併は 12%、糖尿病の合併は除外された。動脈硬化の指標である IMT は、年齢 (R=0.38)、最高血圧 (R=0.23)、最低血圧 (R=0.16)、BMI (R=0.15)、MDA-LDL (R=0.11) と正の相関 (p<0.01)、HDL-C (R=0.23) と負の相関 (p<0.01) を示した。

表 一般住民における頚動脈内膜中膜肥厚度と危険因子の相関

危険因子	R値	P値
年齢	0.377	<0.001
BMI	0.151	<0.001
最高血圧	0.227	<0.001
最低血圧	0.158	<0.001
LDL-C	0.031	0.485
HDL-C	0.234	<0.001
MDA-LDL	0.111	<0.01
TG	0.072	0.102
LDL size	0.082	0.270

E. 研究結果と考察

今回の調査から、頚動脈内膜中膜肥厚度を指標とした動脈硬化の進展には、年齢、肥満度、最高血圧、最低血圧、HDL コレステロール、MDA-LDL が関与することが示唆された。これらの結果は、高脂血症を有する対象において、他の危険因子の重積が動脈硬化の進展をひき起こすことを示唆する。

F. 健康危険情報

特記事項なし

G. 研究発表

論文発表

1:Yamaguchi M, Matsumoto F, Bujo H, Shibasaki M, Takahashi K, Yoshimoto S, Ichinose M, Saito Y. Revascularization determines volume retention and gene expression by fat grafts in mice. Exp Biol Med (Maywood). 2005 Nov;230(10):742-8.

2: Ito M, Bujo H, Takahashi K, Arai T, Tanaka I, Saito Y. Implantation of primary cultured adipocytes that secrete insulin modifies blood glucose levels in diabetic mice. Diabetologia. 2005 Aug;48(8):1614-20.

3: Seki N, Bujo H, Jiang M, Tanaga K, Takahashi K, Yagui K, Hashimoto N, Schneider WJ, Saito Y. LRP1B is a negative modulator of increased migration activity of intimal smooth muscle cells from rabbit aortic plaques. Biochem Biophys Res Commun. 2005 Jun 17;331(4):964-70.

4: Fujita Y, Ezura Y, Bujo H, Nakajima T, Takahashi K, Kamimura K, Iino Y, Katayama Y, Saito Y, Emi M. Association of nucleotide variations in the apolipoprotein B48 receptor gene (APOB48R) with hypercholesterolemia. J Hum Genet. 2005;50(4):203-9.

5: Miyazawa-Hoshimoto S, Takahashi K, Bujo H, Hashimoto N, Yagui K, Saito Y. Roles of degree of fat deposition and its localization on VEGF expression in adipocytes. Am J Physiol Endocrinol Metab. 2005 Jun;288(6):E1128-36.

6: Seki N, Bujo H, Jiang M, Shibasaki M, Takahashi K, Hashimoto N, Saito Y. A potent activator of PPARalpha and gamma reduces the vascular cell recruitment and inhibits the intimal thickning in hypercholesterolemic rabbits. Atherosclerosis. 2005 Jan;178(1):1-7.

H. 知的財産権の出願、登録状況

特になし。

Ⅲ．研究成果の刊行に関する一覧表

雑誌

発表者氏名	論文タイトル名	発表誌名	巻号	ページ	出版年
Yamaguchi M, Matsumoto F, Bujo H, Shibasaki M, Takahashi K, Yoshimoto S, Ichinose M, Saito Y.	Revascularization determines volume retention and gene expression by fat grafts in mice.	Exp Biol Med (Maywood)	230(10)	742-8	2005
Ito M, Bujo H, Takahashi K, Arai T, Tanaka I, Saito Y.	Implantation of primary cultured adipocytes that secrete insulin modifies blood glucose levels in diabetic mice.	Diabetologia	48(8)	1614-20	2005
Seki N, Bujo H, Jiang M, Tanaga K, Takahashi K, Yagui K, Hashimoto N, Schneider WJ, Saito Y.	LRP1B is a negative modulator of increased migration activity of intimal smooth muscle cells from rabbit aortic plaques.	Biochem Biophys Res Commun	331(4)	964-70	2005
Fujita Y, Ezura Y, Bujo H, Nakajima T, Takahashi K, Kamimura K, Iino Y, Katayama Y, Saito Y, Emi M.	Association of nucleotide variations in the apolipoprotein B48 receptor gene (APOB48R) with hypercholesterolemia.	J Hum Genet	50(4)	203-9	2005
Miyazawa-Hoshimoto S, Takahashi K, Bujo H, Hashimoto N, Yagui K, Saito Y.	Roles of degree of fat deposition and its localization on VEGF expression in adipocytes.	Am J Physiol Endocrinol Metab	288(6)	E1128-36	2005
Seki N, Bujo H, Jiang M, Shibasaki M, Takahashi K, Hashimoto N, Saito Y.	A potent activator of PPARalpha and gamma reduces the vascular cell recruitment and inhibits the intimal thickning in hypercholesterolemic	Atherosclerosis	178(1)	1-7	2005
Nakagawa Y-Toyama, Hirano K, Tsujii K, Nishida M, Miyagawa J, Sakai N, and Yamashita S.	Human scavenger receptor class B type I is expressed with cell-specific fashion in both initial and terminal sites of reverse cholesterol	Atherosclerosis.	183	75-83	2005
Zhang Z, Hirano K, Tsukamoto K, Ikegami C, Koseki M, Saijo K, Ohno T, Sakai N, Hiraoka H, Shimomura I,	Defective cholesterol efflux in Werner syndrome fibroblasts and its phenotypic correction by Cdc42, a RhoGTPase.	Exp Geront	40	286-294	2005
Son le NT, Kunii D, Hung NT, Sakai T, Yamamoto S	The metabolic syndrome: prevalence and risk factors in the urban population of Ho Chi Minh	Diabetes Res Clin Pract	67	243-250	2005
Sone H, Tanaka S, Ishibashi S, Yamasaki Y, Oikawa S, Ito H, Saito Y, Ohashi Y, Akanuma Y, Yamada N, Japan Diabetes Complications Study (JDCS) Group.	The new worldwide definition of metabolic syndrome is not a better diagnostic predictor of cardiovascular disease in Japanese diabetic patients than the existing definitions. Additional analysis from the Japan Diabetes Complications	Diabetes Care	29(1)	145-7	2006
Sone H, Mizuno S, Fujii H, Yoshimura Y, Yamasaki Y, Ishibashi S, Katayama S, Saito Y, Ito H, Ohashi Y, Akanuma Y, Yamada N; Japan Diabetes	Is the diagnosis of metabolic syndrome useful for predicting cardiovascular disease in asian diabetic patients? Analysis from the Japan Diabetes Complications Study.	Diabetes Care	28(6)	1463-71	2005
Sone H, Mizuno S, Yamada N.	Vascular risk factors and diabetic neuropathy.	N Engl J Med	352	1925-7	2005
Nakagawa Y, Shimano H, Yoshikawa T, Ide T, Tamura M, Furusawa M, Yamamoto T, Inoue N, Matsuzaka T, Takahashi A, Hasty AH, Suzuki H, Sone H, Toyoshima H, Yahagi N, and Yamada	TFE3 transcriptionally activates hepatic IRS-2, participates in insulin-signaling and , ameliorates diabetes.	Nat Med	12(1)	107-113	2006
Inoue N, Shimano H, Nakakuki M, Matsuzaka T, Nakagawa Y, Yamamoto T, Sato R, Takahashi A, Sone H, Yahagi N, Suzuki H, Toyoshima H, Yamada N.	Lipid Synthetic Transcription Factor SREBP-1a Activates p21WAF1/CIP1, a Universal Cyclin-Dependent Kinase Inhibitor.	Mol Cell Biol	25(20)	8938-47	2005
Amemiya-Kudo M, Oka J, Ide T, Matsuzaka T, Sone H, Yoshikawa T, Yahagi N, Ishibashi S, Osuga JI, Yamada N, Murase T, Shimano H.	SREBPs activate insulin gene promoter directly and indirectly through synergy with BETA2/E47.	J Biol Chem	280(41)	34577-89	2005
Najima Y, Yahagi N, Takeuchi Y, Matsuzaka T, Sekiya M, Nakagawa Y, Amemiya-Kudo M, Okazaki H, Okazaki S, Tamura Y, Iizuka Y, Ohashi K, Harada K, Gotoda T, Nagai R, Kadowaki T, Ishibashi S, Yamada N, Osuga J,	High mobility group protein-B1 interacts with sterol regulatory element-binding proteins to enhance their DNA binding.	J Biol Chem	280(30)	27523-32.	2005
Takahashi A, Shimano H, Nakagawa Y, Yamamoto T, Motomura K, Matsuzaka T, Sone H, Suzuki H, Toyoshima H,	Transgenic mice overexpressing SREBP-1a under the control of the PEPCK promoter exhibit insulin resistance, but not diabetes.	Biochim Biophys Acta	1740(3)	427-33	2005
Suzuki M, Kakuta H, Takahashi A, Shimano H, Tada-Iida K, Yokoo T, Kihara R, Yamada N.	Effects of atorvastatin on glucose metabolism and insulin resistance in KK/Ay mice.	J Atheroscler Thromb	12(2)	77-84	2005

Yahagi N, Shimano H, Hasegawa K, Ohashi K, Matsuzaka T, Najima Y, Sekiya M, Tomita S, Okazaki H, Tamura Y, Iizuka Y, Ohashi K, Nagai R, Ishibashi S, Kadowaki T, Makuuchi M, Ohnishi S, Osuga J, Yamada N.	Co-ordinate activation of lipogenic enzymes in hepatocellular carcinoma.	Eur J Cancer	41(9)	1316-22	2005
Takahashi A, Motomura K, Kato T, Yoshikawa T, Nakagawa Y, Yahagi N, Sone H, Suzuki H, Toyoshima H, Yamada N, Shimano H.	Transgenic mice overexpressing nuclear SREBP-1c in pancreatic beta-cells.	Diabetes	54	492-9	2005
Nakagawa Y, Aoki N, Aoyama K, Shimizu H, Shimano H., Yamada N, Miyazaki H.	Receptor-type protein tyrosine phosphatase epsilon (PTPepsilonM) is a negative regulator of insulin signaling in primary hepatocytes and	Zoolog Sci	22	169-75	2005
Kikuchi H, Kawakami Y, Kakihana K, Kawai K, Murayama Y, Iizuka Y, Suzuki S, Suzuki H, Sone H, Toyoshima H, Shimano H., Yamada N.	Plasma chloride concentration as a new diagnostic indicator of insulin insufficiency.	Diabetes Res Clin Pract	67	137-43	2005
Thu NN, Mai TT, Ohmori R, Kuroki M, Van Chuyen N, Hung NT, Kawakami M, Kondo K,	Effect of the cholesteryl ester transfer protein genotypes on plasma lipid and lipoprotein levels in Vietnamese children.	Pediatr Res	58	1249-53	2005
Yorifuji T, Nagashima K, Kurokawa K, Kawai M, Oishi M, Akazawa Y, Hosokawa M, Yamada Y, Inagaki N, Nakahata T.	The C42R mutation in the Kir6.2 (KCNJ11) gene as a cause of transient neonatal diabetes, childhood diabetes, or later-onset, apparently type 2 diabetes mellitus..	J Clin Endocrinol Metab	90(6)	3174-3178	2005
Kawasaki Y, Taniguchi A, Fukushima M, Nakai Y, Kuroe A, Ohya M, Nagasaka S, Yamada Y, Inagaki N, Seino	Soluble TNF receptors and albuminuria in non-obese Japanese type 2 diabetic patients.	Horm Metab Res	37(10)	617-621	2005
Suzuki H, Fukushima M, Okamoto S, Takahashi O, Shimbo T, Kurose T, Yamada Y, Inagaki N, Seino Y, Fukui T.	Effects of thorough mastication on postprandial plasma glucose concentrations in non-obese Japanese subjects.	Metabolism	54(12)	1593-1599	2005
Mitsui R, Fukushima M, Nishi Y, Ueda N, Suzuki H, Taniguchi A, Nakai Y, Kawakita T, Kurose T, Yamada Y,	Factors responsible for deteriorating glucose tolerance in newly diagnosed type 2 diabetes in Japanese men.	Metabolism	55(1)	53-8	2006
Sassa M, Fukuda K, Fujimoto S, Toyoda K, Fujita Y, Matsumoto S, Okitsu T, Iwanaga Y, Noguchi H, Nagata H, Yonekawa Y, Ohara T, Okamoto M, Tanaka K, M.D., Seino Y, Inagaki N,	A single transplantation of the islets can produce glycemic stability and reduction of basal insulin requirement. Diabetes Res Clin Pract (in press)	Diabetes Res Clin Pract (in press)			
Kayaba K, Tsutsumi A, Gotoh T, Ishikawa S, Miura Y	Five-year stability of job characteristics scale scores among a Japanese working population.	J Epidemiol	15	228-34	2005
石川鎮清、中村好一	自殺者の疫学JMSコホート研究.	厚生の指標	49(15)	16-21.	2002

Ⅳ. 研究成果の刊行物・別冊

Diabetologia (2005) 48: 1614–1620
DOI 10.1007/s00125-005-1825-0

ARTICLE

M. Ito · H. Bujo · K. Takahashi · T. Arai · I. Tanaka · Y. Saito

Implantation of primary cultured adipocytes that secrete insulin modifies blood glucose levels in diabetic mice

Received: 5 January 2005 / Accepted: 9 March 2005 / Published online: 30 June 2005

Abstract *Aim/hypothesis:* In type 1 diabetic patients, basal insulin supplementation plays a central role in tight glycaemic control. Therefore, safe and steady supplementation of basal insulin is strongly desirable, despite the need for multiple injections. The aim of this study was to investigate a procedure for supplementation using genetically engineered, primary-cultured adipocytes in diabetic mice. *Methods:* Furin-cleavable human proinsulin cDNA was transferred into murine primary-cultured adipocytes using a retroviral vector. The cells were implanted subcutaneously into streptozotocin-induced diabetic mice. *Results:* The transfected cells secreted substantial amounts of mature insulin, as well as C-peptide, into conditioned medium. Syngeneic implantation of the cells significantly improved hyperglycaemia and blood HbA_1c concentrations in a manner that was dependent on cell number, without causing hypoglycaemia. The plasma insulin concentration was dependent on the implanted cell number, and the systemic effect of the circulating insulin was confirmed by marked improvement of body weight reduction and liver glycogen content. Additionally, surgical resection of the implants, in which the insulin secretion was immunologically confirmed after transplantation, diminished the glucose-lowering effect, suggesting that in vivo expression could be eliminated if necessary. *Conclusions/interpretation:* These results indicate that the autotransplantation of functionalised adipocytes may lead to a clinical application in the treatment of diabetes.

Keywords Adipocytes · Furin · Glycaemic control · Implantation · Insulin

Abbreviations FBG: fasting blood glucose · GFP: green fluorescent protein · PA: primary adipocyte · s1s2B10-Ins/PA: human proinsulin gene-transfected murine PAs · STZ: streptozotocin

M. Ito · H. Bujo (✉)
Department of Genome Research and Clinical Application,
Graduate School of Medicine,
Chiba University,
1-8-1, Inohana, Chuo-ku,
Chiba, 260-8670, Japan
e-mail: hbujo@faculty.chiba-u.jp
Tel.: +81-43-2227171
Fax: +81-43-2262095

K. Takahashi · Y. Saito
Department of Clinical Cell Biology,
Graduate School of Medicine,
Chiba University,
Chiba, Japan

T. Arai · I. Tanaka
Tsukuba Research Laboratories,
Eisai, Tsukuba, Japan

Introduction

Protein injection therapy is frequently used to treat genetic and acquired protein hormone deficiencies; however, multiple injections remain a major limitation to the lifestyle of these patients. Thus, it would be better for the patients' quality of life to treat with a continuous supplementation system.

Type 1 diabetic mellitus is one of the typical disorders that require multiple injections to prevent various short- or long-term complications [1, 2]. Supplementation of basal insulin, the steady and low level of insulin that is constantly present in the circulation, is central to intensive glucose control; however, an adequate supply is still not easily achieved even with daily multiple injections, due to the occurrence of hypoglycaemia [3]. To overcome this problem, steady-state supplementation of basal insulin is highly desirable [4]. Implantation therapy with ex vivo gene-transferred cells is considered an attractive potential method for continuous insulin supplementation [5]. Moreover, an autotransplantation procedure using self-originated primary cells is highly desirable in order to avoid the need for immunosuppression.

Recently, it has been reported that adipocytes express and secrete various biologically active peptides called adipocytokines [6]. Leptin secreted from adipocytes regulates food intake and energy expenditure [7]. Adiponectin has

been reported to ameliorate insulin resistance in obese mice by enhancement of both fatty acid combustion and energy dissipation in muscle [8]. We have recently reported that 3T3-L1 adipocytes transplanted into the mesenteric area of mice expressed TNF-α, and the cytokine modulated the metabolic status of the recipient mice [9]. These results indicate that adipocytes can secrete bioactive proteins into the blood circulation, and thereby affect the systemic metabolic status. Thus, we hypothesised that adipocytes could be used as a source of protein production in vivo for the modulation of metabolic disorders. Based on the hypothesis, we generated insulin-expressing primary adipocytes (PAs) and evaluated the effect of implantation of these cells in diabetic mice.

Materials and methods

Mice

All mice in this study were obtained from Charles River Japan (Yokohama, Japan). They were allowed free access to regular chow and water unless otherwise specified. All work was carried out according to the guidelines of the Animal Care Committees of Chiba University Graduate School of Medicine and Eisai.

Adipocytes primary culture

PAs were obtained by means of the ceiling culture method reported by Sugihara et al. [10]. Briefly, 0.5–1 g of inguinal s.c. fat was isolated from male 4-week-old C57BL/6 mice. The tissues were minced and digested with collagenases-1 (Nitta Gelatin, Osaka, Japan). The floating layer after centrifugation was seeded into T-25 flasks filled with DMEM (4.5 g/l D-glucose; Sigma, St Louis, MO, USA) supplemented with 10% fetal bovine serum (as normal medium), the flasks placed upside down, and cultured for 2 weeks. The cells attached on the ceiling surface were harvested with trypsin, and grown according to standard procedures.

cDNA isolation

Green fluorescent protein (GFP) cDNA was purchased from BD Biosciences Clontech (Tokyo, Japan). Human preproinsulin gene was amplified with Expand Hi-Fi (Roche Diagnostics KK, Tokyo, Japan) polymerase mixture from a human pancreas cDNA library (BD Biosciences Clontech). The primers were designed as follows: 5′-CATAAGCTT ACCATGGCCCTGTGGATGCGC-3′ (forward, containing a start codon) and 5′-CATTCTAGACTAGTTGCAG TAGTTCTCCAG-3′ (reverse, containing a stop codon). The furin-cleavable modified proinsulin gene [11] (named s1s2B10-Ins in this study) was generated using a Quikchange site-directed mutagenesis kit (Stratagene, La Jolla, CA, USA). The furin-cleavable sites at the B–C junction (as site 1) and the C–A junction (as site 2) were created using the oligomers 5′-CTTCTACACACCCAGGACCA AGCGGGAGGCAGAGGAC-3′ (site 1) and 5′-CCCTGG AGGGATCCCGGCAGAAGCGTGG-3′ (site 2). The resulting substitution of amino acids are as follows: lysine to arginine at amino acid number 29 and arginine to lysine at number 31 in site 1, and leucine to arginine at number 62 in site 2. A mutation of the tenth amino acid in the B-chain (from histidine to aspartic acid) was created using the primer 5′-CACCTGTGCGGATCCGACCT GGTGGAAGC-3′. These modifications were confirmed by sequencing.

Construction of retroviral vectors and gene transduction

In this study, we used the vesicular stomatitis virus G-protein-pseudotyped retroviral vector [12] for stable gene transfer to PAs. The vector structures are shown in Fig. 1a.

Preparation of the pseudotyped vector was largely based on a ViraPort Retroviral Gene Expression System (Stratagene). The retroviral vector was harvested by transfection of the plasmid mixture composed of the ViraPort system and the insulin-expression vector into 293-EBNA cells (Invitrogen, Tokyo, Japan; 2×10^6 cells/10 ml in 100 mm dish) using TransIT (Mirus, Madison, WI, USA). Two days later, the conditioned medium containing vector particles (200 ml) was collected and concentrated by ultracentrifugation (50,000×*g*, 100 min at 4°C). The concentrated vec-

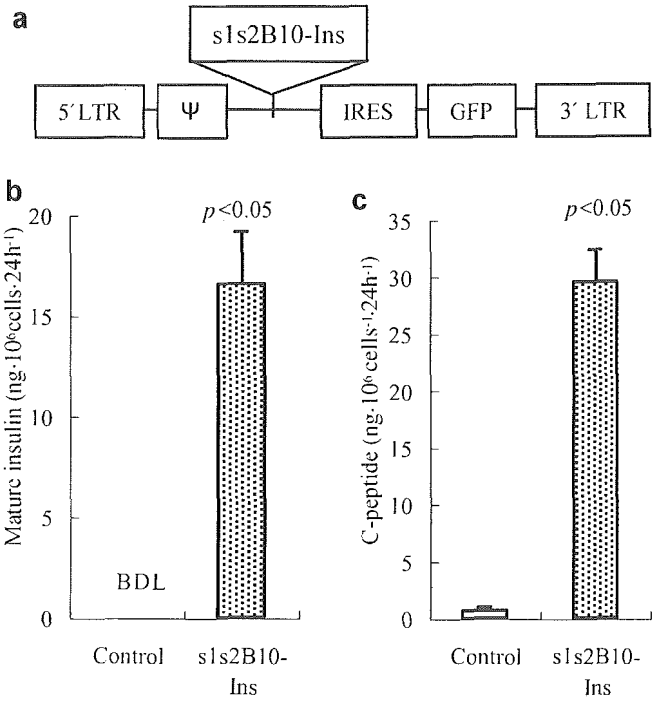

Fig. 1 Transduction to PAs of a retrovirus vector expressing modified human insulin. Gene structure of the retroviral vector (**a**). *ψ* packaging signal sequence. The concentrations of mature insulin (**b**) and C-peptide (**c**) were measured in 24-h-conditioned medium. *IRES* Internal ribosome entry site *LTR* long terminal repeat; *BDL* below the detection limit (0.08 ng/ml in our study)

tor solution was transduced into subconfluent PAs (six-well plates) with 2 μg/ml Polybrene (Sigma). The transduction of retroviral vector containing GFP showed that more than 95% of PAs were transduced with the vector. The reserve cell stocks were cryopreserved with Cellbanker solution (Wako Pure Chemical Industries, Osaka, Japan).

Detection of gene products

In vitro secretion of mature insulin and C-peptide was assayed using ELISA kits from Linco Research (St Charles, MO, USA) and IBL (Gunma, Japan), respectively. All assay procedures were according to the manufacturers. The insulin detection kit is known to detect site-1-undigested proinsulin as well as mature insulin, and not proinsulin or site-2-undigested proinsulin. Taking into account the cross-reactivity of antibodies with the proinsulin in the kit, conversion to mature insulin was expected to about 5% of total secreted insulin.

Implantation of insulin-expressing PAs into streptozotocin-induced diabetic mice

Prior to the experiment using PAs expressing insulin, we examined the implantation of PAs expressing placental alkaline phosphatase as a secretion marker (data not shown). For this purpose, we implanted transplants between individual mice of this strain (syngeneic), because it does not require immunosuppression after transplantation. Based on the results, we confirmed the long-term and stable expression of exogenous genes in PAs, and secretion into the circulation, by implantation of gene-transferred PAs in mice.

Streptozotocin (STZ) (Sigma) was dissolved in 1 mmol/l cold sodium citrate (pH 4.5) just prior to i.v. injection at a dose of 170 mg/kg into the tail vein of 9-week-old male C57BL/6 mice (groups of four to six). Blood samples were collected from the tail vein in a 16-h-fasted state (10.00 hours). The blood glucose levels were determined with a Glucose CII (Wako). Two to three weeks later, mice in which the fasting blood glucose (FBG) levels rose to over 19.4 mmol/l were selected for experiment.

In order to accelerate the differentiation of implanted cells, gene-transferred PAs were treated, prior to implantation, with medium supplemented with 0.5 mmol/l 3-isobutyl-1-methylxanthine, 0.25 μmol/l dexamethasone and 10 μg/ml recombinant human insulin (all from Sigma) for 3 days. The harvested cells were suspended at 2×10^6 cells/ml in Matrigel (BD Biosciences) supplemented with 1 μg/ml recombinant human basic fibroblast growth factor (Genzyme Techne, Minneapolis, MN, USA) and injected s.c. in the back of the mice. FBG and body weight were monitored at 1, 3, 5, 7, 9 and 10 weeks after implantation. At 9 weeks, plasma samples were collected from the retro-orbital venous plexus of mice and plasma insulin concentrations were assayed by an ultrasensitive ELISA (Morinaga, Yokohama, Japan). HbA_1c values at 10 weeks were evaluated with a DCA2000 HbA_1c analyser (Bayer Medical, Tokyo, Japan).

Resection of implanted cells from mice

Cells from cryopreserved stock were used in the study. Implantation (8×10^6 cells/mouse of control PAs or s1s2B10-Ins/PA) and FBG evaluation were performed as described above. Three weeks after implantation, mice were anaesthetised by i.p. administration of sodium pentobarbital (50 mg/kg). Then the implanted area was shaved, the skin incised and the implants removed, followed by suturing and disinfection. The FBG levels were determined 2 weeks after operation; however, direct statistical comparison with control mice could not be performed because they had already died. Since two of three resected mice died at 3 weeks after operation, the plasma concentration of insulin was determined using the remaining resected mouse at 4 weeks after operation.

Histological staining

At 5 weeks after implantation, livers were isolated and sections were embedded in paraffin for a periodic acid–Schiff reaction. The resected implants were collected, fixed in 10% buffered formalin and embedded in paraffin for haematoxylin/eosin staining.

Immunohistochemical staining of insulin in fixed implants was done using guinea-pig anti-human insulin antibody (Linco Research) with EnVision plus reagent (Dako Cytomation, Kyoto, Japan), as recommended by the manufacturers.

Statistical analysis

Data are expressed as means±SEM. Statistical analysis was conducted using the software package SAS 8.1 (SAS Institute Japan, Tokyo, Japan). In animal studies, the evaluation was performed by one-way ANOVA, followed by a Dunnett-type multiple comparison test with the control. The results of ELISA were evaluated with the Mann–Whitney U-test. A value of $p<0.05$ was considered significant.

Results

In vitro expression of modified insulin from PAs

A retroviral vector that expressed modified insulin was constructed as shown in Fig. 1a. The mature insulin production in conditioned medium of s1s2B10-Ins/PA was 16.6±2.59 ng·10^6 cells^{-1}·24 h^{-1} (Fig. 1b). The marked increase of C-peptide suggested successful processing by furin in the adipocytes (Fig. 1c). The biological activity of

engineered insulin was confirmed by autophosphorylation activity against endogenous insulin receptor in HepG2 cell (data not shown).

Implantation of insulin-expressing PAs ameliorated hyperglycaemia

Diabetic mice were created by administration of STZ. Implantation of s1s2B10-Ins/PA significantly lowered the blood glucose levels in the fasting state, this reduction being dependent on cell number (Fig. 2). In mice implanted with 8×10^6 cells of s1s2B10-Ins/PA (high-cell-number group), FBG levels were close to the normal range through the experimental period (10 weeks) without the occurrence of hypoglycaemia in the fasting state.

Plasma insulin concentrations in implanted mice were determined at 9 weeks (Fig. 3). In the high-cell-number group, in which the average FBG level was controlled to a normal level, plasma insulin was significantly increased (160±55 pg/ml, $p<0.05$) compared with the control group (below the detection limit). The value in the low-cell-number group (4×10^6 cells of s1s2B10-Ins/PA) was not significantly different from the control ($p=0.058$), but was nevertheless elevated to nearly half that of the high-cell-number group (92.0±38.1 pg/ml), indicating that the lowering effect on FBG is cell-number-dependent.

Subcutaneous implantation improved systemic metabolic status

To assess the systemic effects of insulin from implants, we analysed liver glycogenesis by the periodic acid–Schiff reaction (Fig. 4). In accord with previous studies [13, 14], STZ treatment caused depletion of liver glycogen. Subcutaneous implantation of s1s2B10-Ins/PA dramatically increased the glycogen content.

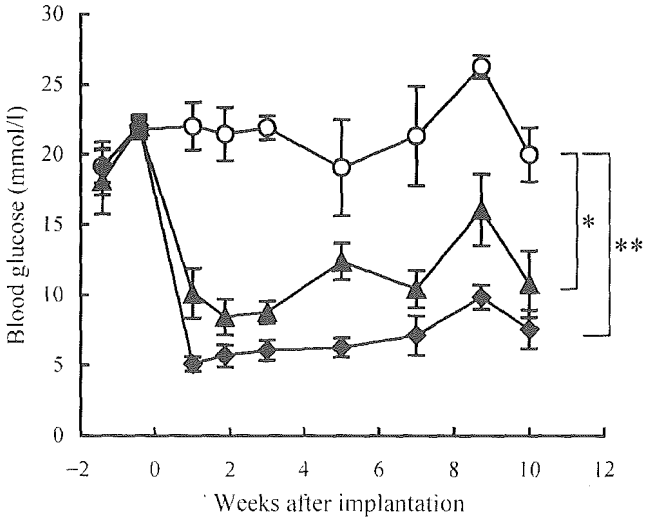

Fig. 2 FBG levels of s1s2B10-Ins/PA-implanted STZ mice. Implantation of control cells (*open circle*, $n=6$), or a low cell number (*solid triangle*, 4×10^6 cells/mouse, $n=5$) and high cell number (*solid diamond*, 8×10^6 cells/mouse, $n=4$) of s1s2B10-Ins/PA cells was performed at day 17 after STZ administration. $*p<0.05$; $**p<0.01$ vs control

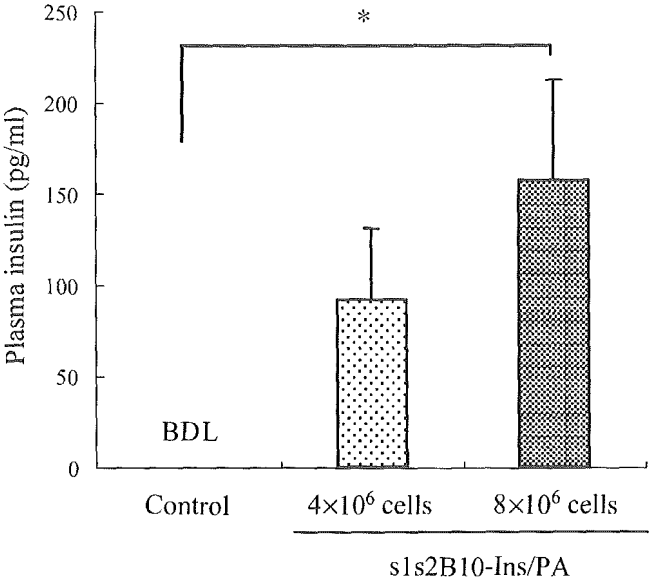

Fig. 3 Plasma insulin concentrations in implanted mice. Eight weeks after implantation, plasma samples were collected and the concentration of insulin determined. The values in plasma from all control mice were below the detection limit (BDL, 50 pg/ml in our assay). Data are means±SEM of four mice (control and high cell number of s1s2B10-Ins/PA) or five mice (low cell number of s1s2B10-Ins/PA). $*p<0.05$

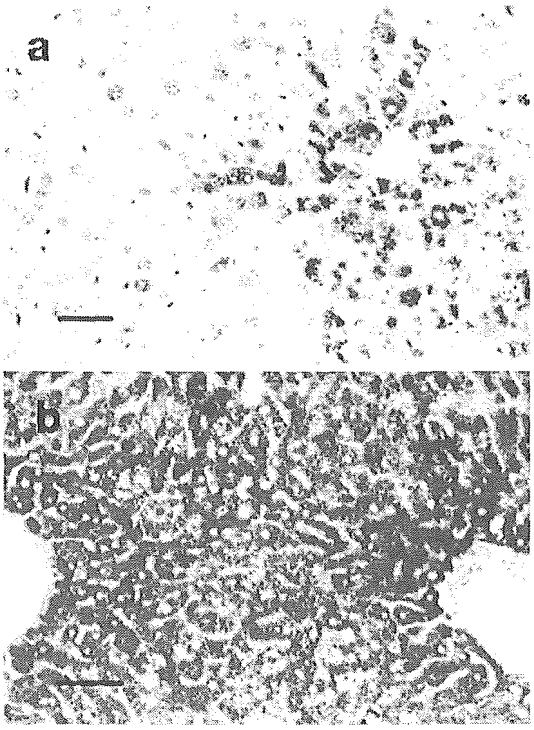

Fig. 4 Liver glycogen contents in implanted mice. The liver sections isolated from killed animals were stained for glycogen. **a** Control-cell-implanted mice. **b** s1s2B10-Ins/PA-implanted mice. *Scale bar*=100 μm

The systemic effect of the implantation was also confirmed by an improvement of body weight loss. The values were significantly different in s1s2B10-Ins/PA groups compared with control from 1 week, and the effects were sustained to the end of the study. The values at 10 weeks were 21.7±0.5 g in the high-cell-number group ($p<0.001$), 19.7±0.4 g in the low-cell-number group ($p<0.01$) and 16.5±0.9 g in the control group.

In order to examine the quality of glycaemic control by the implantation, HbA_1c concentration was determined at the end of the experimental period. In comparison with control mice (9.8±0.7%), the HbA_1c value was significantly lowered in the high-cell-number group (8.4±0.5%, $p<0.01$).

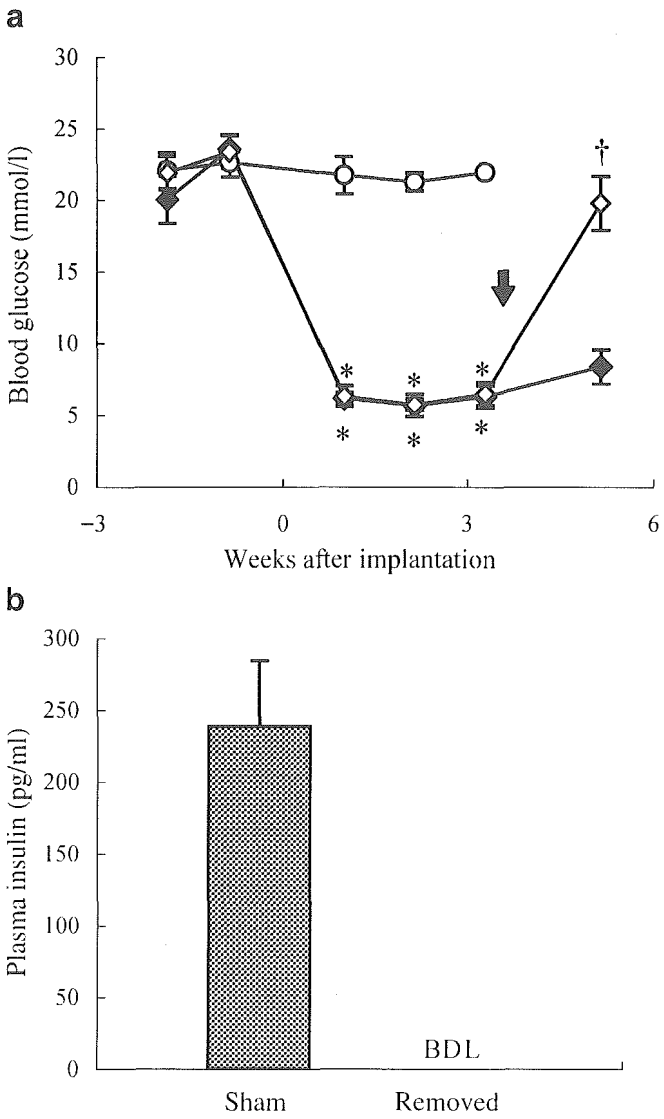

Fig. 5 Resection of the implants diminished the glucose-lowering effect and plasma insulin concentration in mice. **a** FBG levels. Implantation of control cells (*open circle*, $n=6$) or s1s2B10-Ins/PA was performed as shown in Fig. 3. In s1s2B10-Ins/PA-implanted mice, the gross implants were removed surgically (*open diamond*, $n=3$) at 3 weeks after implantation (*arrow*). A sham operation was performed in the non-resected group (*solid diamond*, $n=6$). **b** Plasma insulin concentration at 5 weeks after implantation. The value in control mice was below the detection limit (BDL, 50 pg/ml in our assay). $^*p<0.01$ vs control; $^\dagger p<0.01$ vs the sham-operated group

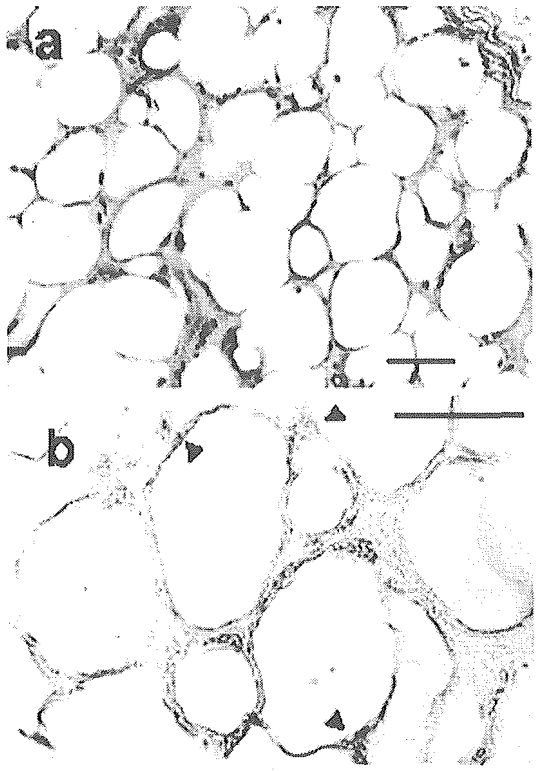

Fig. 6 Tissue staining of resected implants from mice. **a** Haematoxylin/eosin stain. **b** Immunohistochemistry with anti-human insulin IgG. *Arrowheads* indicate typical insulin-positive areas. *Scale bars*=100 μm

Reversal of the glucose-lowering effect by resection

One advantage of our procedure lies in the possibility of resection of the implants in the case of adverse effects and/or over-reaction, such as hypoglycaemia. We studied the effect of removal of the implants from treated STZ mice. FBG levels after surgical resection of the implants significantly increased from those of sham-operated mice, and reached almost the level seen previously in the control mice (Fig. 5a). Plasma insulin was dramatically reduced by the operation (Fig. 5b).

Finally, we identified the insulin-positive cells in the implants. Histological and immunohistochemical analysis showed that insulin-positive cells existed in implants as mature adipocytes, which seemed to store lipid droplets (Fig. 6). No positive signal was obtained with control IgG (data not shown).

Discussion

The majority of systemic protein deficiencies are currently treated by multiple injections of the lacking polypeptide. Safe administration procedures that would eliminate this unpleasant duty are highly desirable. In this report, we have

established the procedure for in vivo gene expression based on gene-transferred PAs using type 1 diabetes model mice. We confirmed that protein secretion from s.c. implanted cells could improve metabolic status systemically (e.g. in liver, shown in Fig. 4). Furthermore, as shown in Fig. 5, the glucose-lowering effects were retained when the cryopreserved cells were used, suggesting that sufficient cells for repeated implantations during clinical treatment might be obtainable by growth from stable reserve stocks. From these results, autotransplantation of gene-transferred PAs is thought to be an attractive candidate method for our aim.

A similar approach using self-originated adipocytes might be applicable for humans. Isolation of human fat tissue is being established as liposuction in plastic surgery and cosmetic surgery [15, 16]. Human PAs can also be obtained by ceiling culture [17]. Our investigations may thus provide a basis for the treatment of patients by long-term supplementation of therapeutic protein without systemic immunosuppression.

Supplementation of basal levels of insulin is known to act not only centrally for adequate control of hyperglycaemia, but also has a key role in preventing the development of ketoacidosis in humans [18]. In our study, sustained insulin supplementation from implants successfully lowered blood glucose in a manner that was dependent on cell number, suggesting that the procedure might make it possible to achieve long-term, steady-state insulin supplementation without the need for multiple injections. Therefore, it could be particularly helpful for elderly patients or patients with impaired vision, who find such injections hard to administer by themselves. Implantation of the s1s2B10-Ins/PA is also thought to supply C-peptides (Fig. 1c), which are not provided by the usual insulin injections. Since the peptides have been reported to have a protective effect on microvascular complications [19–21], the implantation might contribute to prevention of such complications. Moreover, removal of the implants reversed the glucose-lowering effect, suggesting that in vivo expression of insulin generated in this way could be surgically eliminated if necessary.

Recently, a long-acting human insulin analogue has been developed and is reported to improve hyperglycaemia and HbA_1c levels in type 1 [22] and type 2 diabetic patients [23]. These results suggest that a sustained supply of basal insulin is effective clinically in both forms of diabetes.

In our experiment, a single implantation retained its glucose-lowering effect for several months without causing hypoglycaemia. Previous trials showed hypoglycaemia at 3–4 weeks due to unregulated cell proliferation in vivo, resulting in increased insulin production [24, 25]. We speculate that the apparent advantage of PAs is due to their ability to differentiate, since the implanted PAs existed as mature adipocytes in the implants as assessed by histological analysis (Fig. 5).

This unproliferative property of implanted PAs may also contribute to safety if the procedure is applied to clinical treatment. Recently, it was reported that retrovirus-mediated gene transfer could cause uncontrolled T-cell proliferation in clinical trials for SCID-X1 [26]. This proliferation is thought to be triggered by retrovirus vector insertion in proximity to the LIM domain only-2 proto-oncogene promoter. However, it is expected that such aberrant proliferation could be minimised by our strategy of using PAs because of the containment and removability of the cells.

In summary, this is the first report that syngeneic implantation of gene-transferred PAs has successfully improved a systemic disorder in mice. This approach might be useful clinically for the treatment of patients with diabetes and other disorders caused by loss of circulating polypeptide(s).

Acknowledgements These studies were supported by grants from the Japanese Ministry of Education, Science, Sports and Culture to H. Bujo and Y. Saito.

References

1. The Diabetes Control and Complications Trial Research Group (1993) The effect of intensive treatment of diabetes on the development and progression of long-term complications in insulin-dependent diabetes mellitus. N Engl J Med 329:977–986
2. UK Prospective Diabetes Study (UKPDS) Group (1998) Intensive blood-glucose control with sulphonylureas or insulin compared with conventional treatment and risk of complications in patients with type 2 diabetes (UKPDS 33). Lancet 352:837–853
3. The Diabetes Control and Complications Trial Research Group (1997) Hypoglycemia in the diabetes control and complications trial. Diabetes 46:271–286
4. Barnett AH (2003) A review of basal insulins. Diabet Med 20:873–885
5. Bailey CJ, Davies EL, Docherty K (1999) Prospects for insulin delivery by ex-vivo somatic cell gene therapy. J Mol Med 77:244–249
6. Shimomura I, Funahashi T, Takahashi M et al (1996) Enhanced expression of PAI-1 in visceral fat: possible contributor to vascular disease in obesity. Nat Med 2:800–803
7. Zhang Y, Proenca R, Maffei M, Barone M, Leopold L, Friedman JM (1994) Positional cloning of the mouse obese gene and its human homologue. Nature 372:425–432
8. Yamauchi T, Kamon J, Waki H et al (2001) The fat-derived hormone adiponectin reverses insulin resistance associated with both lipoatrophy and obesity. Nat Med 7:941–946
9. Shibasaki M, Takahashi K, Itou T et al (2002) Alterations of insulin sensitivity by the implantation of 3T3-L1 cells in nude mice. A role for TNF-alpha? Diabetologia 45:518–526
10. Sugihara H, Yonemitsu N, Miyabara S, Yun K (1986) Primary cultures of unilocular fat cells: characteristics of growth in vitro and changes in differentiation properties. Differentiation 31:42–49
11. Groskreutz DJ, Sliwkowski MX, Gorman CM (1994) Genetically engineered proinsulin constitutively processed and secreted as mature, active insulin. J Biol Chem 269:6241–6245
12. Arai T, Takada M, Ui M, Iba H (1999) Dose-dependent transduction of vesicular stomatitis virus G protein-pseudotyped retrovirus vector into human solid tumor cell lines and murine fibroblasts. Virology 260:109–115
13. Muzzin P, Eisensmith RC, Copeland KC, Woo SL (1997) Hepatic insulin gene expression as treatment for type 1 diabetes mellitus in rats. Mol Endocrinol 11:833–837
14. Dong H, Morral N, McEvoy R, Meseck M, Thung SN, Woo SL (2001) Hepatic insulin expression improves glycemic control in type 1 diabetic rats. Diabetes Res Clin Pract 52:153–163

15. Vogt PA (1989) Abdominal lipoplasty technique. Clin Plast Surg 16:279–288
16. Markey AC (2001) Liposuction in cosmetic dermatology. Clin Exp Dermatol 26:3–5
17. Zhang HH, Kumar S, Barnett AH, Eggo MC (2000) Ceiling culture of mature human adipocytes: use in studies of adipocyte functions. J Endocrinol 164:119–128
18. Madsbad S, Alberti KG, Binder C et al (1979) Role of residual insulin secretion in protecting against ketoacidosis in insulin-dependent diabetes. Br Med J 2:1257–1259
19. Johansson BL, Kernell A, Sjoberg S, Wahren J (1993) Influence of combined C-peptide and insulin administration on renal function and metabolic control in diabetes type 1. J Clin Endocrinol Metab 77:976–981
20. Ido Y, Vindigni A, Chang K et al (1997) Prevention of vascular and neural dysfunction in diabetic rats by C-peptide. Science 277:563–566
21. Sjoquist M, Huang W, Johansson BL (1998) Effects of C-peptide on renal function at the early stage of experimental diabetes. Kidney Int 54:758–764
22. Pieber TR, Eugene-Jolchine I, Derobert E (2000) Efficacy and safety of HOE 901 versus NPH insulin in patients with type 1 diabetes. The European study group of HOE 901 in type 1 diabetes. Diabetes Care 23:157–162
23. Rosenstock J, Schwartz SL, Clark CM Jr, Park GD, Donley DW, Edwards MB (2001) Basal insulin therapy in type 2 diabetes: 28-week comparison of insulin glargine (HOE 901) and NPH insulin. Diabetes Care 24:631–636
24. Kawakami Y, Yamaoka T, Hirochika R, Yamashita K, Itakura M, Nakauchi H (1992) Somatic gene therapy for diabetes with an immunological safety system for complete removal of transplanted cells. Diabetes 41:956–961
25. Falqui L, Martinenghi S, Severini GM et al (1999) Reversal of diabetes in mice by implantation of human fibroblasts genetically engineered to release mature human insulin. Hum Gene Ther 10:1753–1762
26. Hacein-Bey-Abina S, Von Kalle C, Schmidt M et al (2003) LMO2-associated clonal T cell proliferation in two patients after gene therapy for SCID-X1. Science 302:415–419

Am J Physiol Endocrinol Metab 288: E1128–E1136, 2005.
First published December 21, 2004; doi:10.1152/ajpendo.00003.2004.

Roles of degree of fat deposition and its localization on VEGF expression in adipocytes

Saori Miyazawa-Hoshimoto,[1] Kazuo Takahashi,[1] Hideaki Bujo,[2] Naotake Hashimoto,[3] Kazuo Yagui,[1] and Yasushi Saito[1]

Departments of [1]Clinical Cell Biology, [2]Genome Research and Clinical Application, and [3]Division of Applied Translational Research, Graduate School of Medicine, Chiba University, Chiba, Japan

Submitted 5 January 2004; accepted in final form 17 December 2004

Miyazawa-Hoshimoto, Saori, Kazuo Takahashi, Hideaki Bujo, Naotake Hashimoto, Kazuo Yagui, and Yasushi Saito. Roles of degree of fat deposition and its localization on VEGF expression in adipocytes. *Am J Physiol Endocrinol Metab* 288: E1128–E1136, 2005. First published December 21, 2004; doi:10.1152/ajpendo.00003.2004.—Vascular endothelial growth factor (VEGF) is an important angiogenic factor and is expressed in wide variety of cell types. In this study, we investigated the mechanism of VEGF production in adipocytes in three sets of experiments. First, to clarify the relation between plasma VEGF concentrations and their expressions in adipose tissues, we investigated the genetically obese *db/db* and KK-A^y mice. Plasma VEGF concentrations in obese mice were significantly higher than in control and were related to adiposity. VEGF expressions in visceral fat were enhanced during growth and were related to fat deposition. Next, to demonstrate the relation between VEGF production and lipid accumulation in adipocytes, we analyzed VEGF mRNA expression and its protein secretion in 3T3-L1 cells. VEGF production was enhanced during lipid accumulation in 3T3-L1 cells after adipocyte conversion. Next, to clarify the role of anatomic localization on VEGF expression in adipocytes, we implanted 3T3-L1 cells into visceral or subcutaneous fat in athymic mice. 3T3-L1 cells implanted into the mesenteric area expressed more VEGF mRNA than that into the subcutaneous area. Plasma VEGF concentration in the mice implanted in visceral fat was higher than in controls. These results suggest that both the anatomic localization and the lipid accumulation are important for the VEGF production in adipocytes.

vascular endothelial growth factor; fat distribution; cytokine; gene expression; 3T3-L1 cells

VASCULAR ENDOTHELIAL GROWTH FACTOR (VEGF) is a very potent angiogenic factor that induces migration and proliferation of vascular endothelial cells (9). VEGF also enhances vascular permeability and modulates thrombogenicity (18). It has therefore been implicated in normal blood vessel development as well as in pathological vessel formation (6). Pathogenic neovascularization plays a major role in the development of atherosclerosis (20), tumor growth (18), rheumatoid arthritis (9, 16), and various retinopathies (2, 3). VEGF mRNA expression has been identified in various cell types, including endothelial, epithelial, and mesenchymal cells (9, 18). It has also been reported that VEGF mRNA is expressed in 3T3-F442A cells, an established preadipocyte cell line (4).

VEGF is encoded by a single gene; however, four isoforms of 205, 188, 164, and 120 amino acids long are produced as a result of alternative splicing. The 164-amino acid-long isoform is the most abundant. We have reported that serum concentration of the 164-amino acid-long isoform of VEGF in human obese subjects is dependent on the intra-abdominal fat accumulation determined using computed tomography scan at the umbilical level (15). Furthermore, the elevated VEGF level or the accumulated visceral fat in the obese subjects was decreased after body weight reduction (15). These observations revealed that the VEGF secretion from adipose tissues, particularly from visceral adipose tissues, might regulate its serum concentration.

Adipose tissues have been reported to express and release various secretary molecules, such as leptin (10, 11), tumor necrosis factor-α (TNF-α) (7), plasminogen activator inhibitor-1 (PAI-1) (20), and IL-6 (22). Especially, the expression levels of TNF-α and PAI-1 in adipocytes are shown to be directly related to the degree of differentiation from preadipocytes and to be dependent on their anatomic location (12, 14, 20, 21).

Therefore, it is very important to clarify the mechanism of VEGF production in adipocytes from the point of view of the adipocyte differentiation process and the site of fat accumulation. In this study, we examined VEGF production from intrinsic adipocytes in *db/db* and KK-A^y mice during growth, from 3T3-L1 cells depending on the differentiation in culture, and from 3T3-L1 cells that were implanted into the visceral or subcutaneous fat area.

MATERIALS AND METHODS

Materials. MCDB131, FBS, and trypsin were purchased from Invitrogen (Carlsbad, CA). PBS was from Nissui Pharmaceuticals (Tokyo, Japan). DMEM, human insulin, dexamethasone, and 3-isobutyl-1-methylxanthine were obtained from Sigma-Aldrich (St. Louis, MO). Collagenase-S1 was from Nitta Gelatin (Osaka, Japan). Growth Factor Reduced BD Matrigel matrix was from Nippon Becton-Dickinson (Tokyo, Japan). ISOGEN reagent was from NIPPON GENE (Tokyo, Japan). RNeasy Mini Kits and QIAGEN OneStep RT-PCR Kit were from Qiagen (Tokyo, Japan). 3T3-L1 cells, an established preadipocyte cell line, was obtained from the American Type Culture Collection (Manassas, VA). Human umbilical vein endothelial cells (HUVECs) and EBM-2 medium were from BioWhittaker (Walkersville, MD).

Obese mice. BKS.Cg-+ Lepr^{db}/+ Lepr^{db}/Jcl (*db/db*) and KK-A^y/TaJcl (KK-A^y) mice, and control littermates BKS.Cg-m +/+ Lepr^{db}/Jcl (*db/+*) and C57BL/6JJcl (C57BL/6), respectively, were obtained from CLEA Japan (Tokyo, Japan) at 5 wk of age. The mice were maintained in a temperature-, humidity-, and light-controlled room (12:12-h light-dark cycle) with free access to water and standard

Address for reprint requests and other correspondence: K. Takahashi, Dept. of Clinical Cell Biology, Graduate School of Medicine, Chiba University, 1-8-1 Inohana, Chuo-ku, Chiba 260–0856, Japan.

The costs of publication of this article were defrayed in part by the payment of page charges. The article must therefore be hereby marked "*advertisement*" in accordance with 18 U.S.C. Section 1734 solely to indicate this fact.

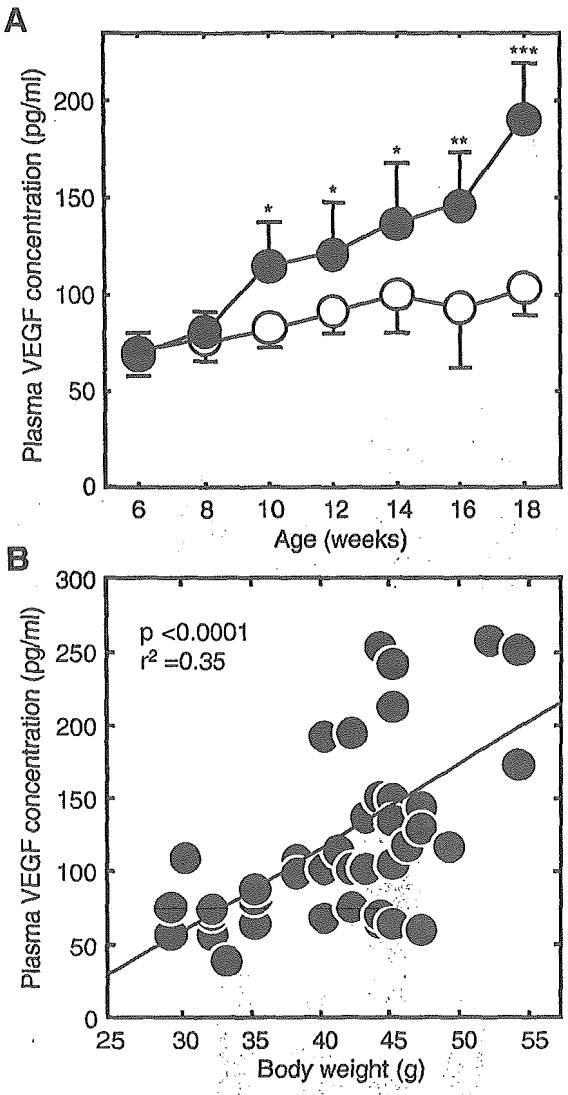

Fig. 1. Growth-dependent change of plasma vascular endothelial growth factor (VEGF) concentration in *db/db* mice. *A*: time course changes of plasma VEGF concentrations in *db/db* (●) and *db/+* (○) mice. Plasma VEGF concentrations were measured every 2 wk from 6 to 18 wk of age in *db/db* and *db/+* mice. Results are represented as means and SD. After 10 wk of age, plasma VEGF concentrations in *db/db* mice were significantly higher than in *db/+* mice. *B*: correlation between body weight and plasma VEGF concentrations in *db/db* mice. Plasma VEGF concentrations were significantly correlated with body weight in *db/db* mice. $^{*}P < 0.05$ vs. *db/+* mice; $^{**}P < 0.01$ vs. *db/+* mice; $^{***}P < 0.001$ vs. *db/+* mice.

rodent chow (352 kcal/100 g, CE-2; CLEA Japan). Male mice were used in the studies reported here. Animal care and procedures were approved by the Animal Care Committee of Chiba University School of Medicine.

Body weight and adiposity. Body weights of *db/db* and *db/+* mice were measured at every 2 wk from the time they were 6 wk old throughout the study. Blood samples were also obtained from the retroorbital venous plexus of the mice fasted more than 16 h. The *db/db* and *db/+* mice were killed at 6, 10, 14, and 18 wk of age by cervical dislocation before white adipose tissues were collected. Mesenteric adipose tissues were used as visceral fat, and inguinal subcutaneous adipose tissues were used as subcutaneous fat in the studies reported here. The white adipose tissues were weighed on an analytic balance and processed for cell counts as described previously (13). Briefly, minced adipose tissues were incubated with PBS containing collagenase S-1. The tissue fragments were removed by passage through a 250-μm nylon screen. The isolated cells were then stained with methylene blue, and aliquots were placed on a Neubauer hemocytometer. Total cell counts were measured using a light microscope.

Total RNA and protein extraction from adipose tissues in obese mice. Mesenteric and subcutaneous adipose tissues of *db/db* and *db/+* mice were processed for total RNA isolation using ISOGEN reagents according to the manufacture's instructions. In another set of experiments, the adipose tissues were homogenized in an ice-cold buffer containing 50 mM Tris·HCl (pH 7.4), 1 mM EDTA, 1 mM dithiothreitol, 5 mM $MgCl_2$, 130 mM NaCl, 1% NP-40, 10 μM 4-amidinophenylmethanesulfonyl fluoride, and 5 μM leupeptin. Insoluble materials in the tissue were removed by centrifugation at 12,000 *g* at 4°C for 20 min. After centrifugation, tissue extracts were collected. Moreover, total RNA in the isolated adipocytes of mesenteric fat was also prepared. The mesenteric adipose tissue was digested with collagenase S-1 and passed through a 250-μm nylon screen to remove tissue debris. Then, the isolated cells, containing adipocytes and vascular-stromal cells, were separated by centrifugation. After the adipocytes were allowed to float, the vascular-stromal cells were removed from the bottom layer. The floating layer, as adipocyte fraction, was washed three times with PBS. Finally, the isolated adipocytes were collected and processed for cell counts, using a Neubauer chamber as described above. To compare directly the cellular expression of VEGF in adipocyte, 2×10^4 cells were processed for total RNA isolation using ISOGEN reagent. The KK-A^y and C57BL/6 mice were killed at 16 wk of age by cervical dislocation before mesenteric and inguinal subcutaneous fat was collected for total RNA isolation.

3T3-L1 cells culture and differentiation. 3T3-L1 preadipocytes were cultured with DMEM containing 10% FBS at 37°C in a 5% CO_2 incubator. Adipocyte differentiation was carried out by changing to a differentiation medium containing 10 μg/ml insulin, 0.25 μM dexamethasone, and 0.5 mM 3-isobutyl-1-methylxanthine. After 48 h, the medium was replaced with a maturation medium containing 5 μg/ml insulin, and cells were maintained in this medium until use. Every week after differentiation, the cells were washed with PBS and then cultured in fresh DMEM medium alone. After incubation for 24 h, the conditioned media were collected. In another set of experiments, the cells were processed for total RNA isolation using an RNeasy Mini Kit.

In vitro endothelial tube formation assay. HUVECs were grown in EBM-2 medium containing 10% FBS. Formation of capillary tube-like structures by HUVECs was assessed in a Matrigel-based assay as previously described (8). Briefly, HUVECs were incubated with MCDB131 containing 2% FBS for 48 h prior to tube formation assay. Cells (7×10^4) were plated onto 300 μl of Growth Factor Reduced BD Matrigel matrix (7 mg/ml protein), pregelled at 37°C in 24-well culture plates. Then, the cells were incubated for 13 h at 37°C with 150 μl of MCDB131 and 150 μl of the conditioned medium derived from pre- or postdifferentiated 3T3-L1 cells in the presence or absence of anti-mouse VEGF-neutralizing antibody. Three different phase-contrast microscopic low-power fields (×100) per well were photographed. The total length of capillary tubes in each photograph was measured using a scale ruler.

Preadipocyte transplantation. 3T3-L1 cells were implanted into athymic mice as described previously (19). Briefly, 3T3-L1 preadipocytes were grown to near confluence, trypsinized, and suspended in DMEM with 10% FBS. After centrifugation, cell pellets were resuspended in PBS and injected 1×10^7 cells (500 μl) through 22-gauge needles into the mesenteric area near the small intestine or the subcutaneous fat area of athymic mice of the BALB/C strain under

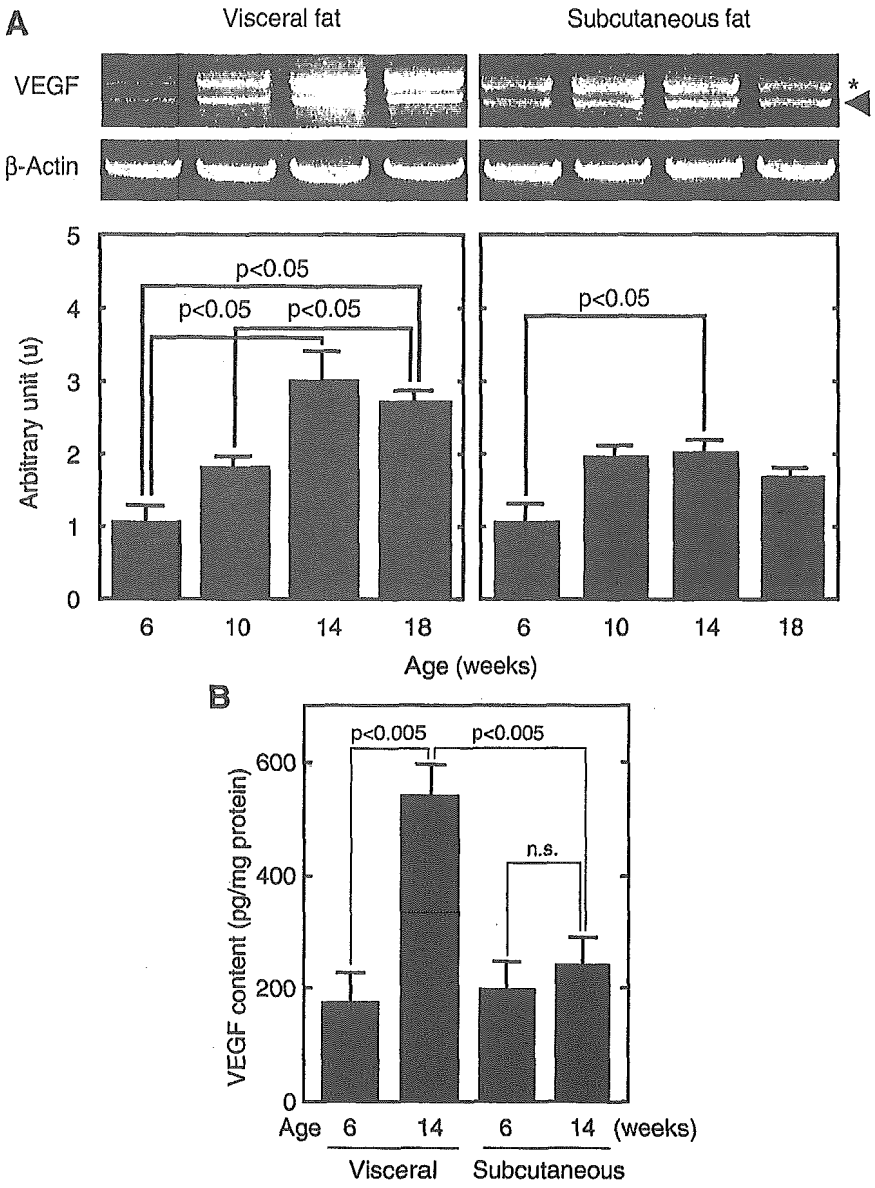

Fig. 2. Growth-dependent changes of mRNA expressions and protein contents of VEGF in mesenteric and subcutaneous adipose tissues of *db/db* mice. *A*: Time course changes of VEGF gene expressions in visceral and subcutaneous adipose tissues of *db/db* mice. Images show RT-PCR products of VEGF amplified from total RNA in mesenteric and subcutaneous adipose tissues at 6, 10, 14, and 18 wk after birth. PCR products of VEGF were densitometrically analyzed, and relative amounts at 6 wk old were set to 1.0. Results are represented as means and SD. Arrowhead, 644 bp ($VEGF_{164}$); *, 716 bp ($VEGF_{188}$). *B*: Tissue VEGF contents in mesenteric and subcutaneous fat. Tissues were extracted with a buffer containing 50 mmol/l Tris·HCl (pH 7.4), 1 mmol/l EDTA, 1 mmol/l DTT, 5 mmol/l $MgCl_2$, 130 mmol/l NaCl, 1% NP-40, 10 μmol/l APMSF, and 5 μmol/l leupeptin. Tissue extracts were processed for VEGF measurement using an ELISA system.

anesthetization by intraperitoneal injection with pentobarbital sodium. Mice were housed in microisolator cages under specific pathogen-free conditions during whole experiments. Four weeks after implantation, the mice were killed by cervical dislocation under anesthetization before mesenteric or subcutaneous fat area was collected. Total RNA of mesenteric and subcutaneous fat was isolated using ISOGEN reagent. Blood samples were also obtained from the retroorbital venous plexus of the mice fasted more than 16 h.

Measurement of immunoreactive VEGF. Plasma samples were prepared by centrifugation at 1,500 *g* for 15 min at 4°C. After centrifugation, the plasma fraction was collected and stored at −70°C until use. The extracts of adipose tissues and the conditioned media from pre- and postdifferentiated 3T3-L1 cells were also stored at −70°C until use. VEGF concentrations of plasma, extracts from adipose tissues, and conditioned media were measured with an enzyme-linked immunosorbent assay system (R&D Systems, Minneapolis, MN).

RT-PCR. To evaluate the contents of VEGF expression in adipose tissues and 3T3-L1 cells, 0.4 μg of total RNA was amplified by OneStep RT-PCR kit using the indicated specific primers. To compare directly the VEGF expressions in adipocytes of mesenteric fat during growth, total RNA prepared from 2×10^4 cells was also amplified using the specific primers. The contents of GLUT4, peroxisome proliferator-activated receptor-γ (PPARγ), and β-actin were also amplified by RT-PCR. The RT-PCR products were run on 1.5% agarose and stained with ethidium bromide. The relative signal intensities of the PCR products were determined with luminescent image analyzer LAS-1000 (Fuji Photo Film, Tokyo, Japan). mRNA amounts were normalized to levels of β-actin mRNA, which served as endogenous standard.

Primers. The following primers were designed for RT-PCR analysis using in this study: VEGF, 5′-GCGGGCTGCCTCGCAGTC-3′ (forward) and 5′-TCACCGCCTTGGCTTGTCAC-3′ (reverse); β-actin, 5′-TGGAATCCTGTGGCATCCATGAAAC-3′ (forward) and 5′-TAAAACGCAGCTCAGTAACAGTCCG-3′ (reverse); GLUT4, 5′-GGCATGTGTGGCTGTGCCATC-3′ (forward) and 5′-GGGTTTCACCTCCTGCTCTAA-3′ (reverse); PPARγ, 5′-GACATCCAA-

GACAACCTGCTG-3′ (forward) and 5′-GCAATCAATAGAAG-GAACACG-3′ (reverse). RT-PCR products for VEGF were 716 bp ($VEGF_{188}$), 644 bp ($VEGF_{164}$), and 512 bp ($VEGF_{120}$), respectively. The signal intensity of the 644-bp product was analyzed in this study. Products of 349, 413, and 258 bp were predicted for β-actin, GLUT4, and PPARγ, respectively.

Statistical analysis. Statistical analyses were performed using Statview J-4.5. Statistical analysis was performed with a *t*-test. All of the results reported herein were confirmed by repeating the experiments with different occasions. A value of $P < 0.05$ indicated statistical significance.

RESULTS

Growth-dependent changes of plasma VEGF concentration in db/db mice. We measured circulating VEGF concentrations in *db/db* mice, a strain of the mouse models for obesity, to demonstrate the role of fat accumulation and its effect on VEGF levels in vivo. Plasma VEGF concentrations were increased during growth in both *db/+* and *db/db* mice (Fig. 1*A*). At 10 wk old, plasma VEGF concentrations in *db/db* mice were significantly higher than in *db/+* mice. Moreover, plasma VEGF concentrations were significantly correlated with body weight (Fig. 1*B*).

Growth-dependent changes of VEGF mRNA expressions and protein contents in visceral and subcutaneous fat of db/db mice. VEGF mRNA was detected in both visceral and subcutaneous fat in *db/db* mice. Expression levels of VEGF mRNA in visceral fat were increased 3.0-fold in 14-wk-old mice compared with those in 6-wk-old mice (Fig. 2*A*). VEGF expressions in subcutaneous fat were also increased during growth, but its enhancement was smaller than in visceral fat. Moreover, tissue contents of VEGF in visceral fat were significantly increased in 14-wk-old mice compared with those in 6-wk-old mice (Fig. 2*B*). However, the VEGF contents in subcutaneous fat were almost the same in 6- and 14-wk-old mice. These data suggest that an enhanced expression of the VEGF gene in visceral fat mainly contributes to the elevated plasma concentrations.

Effect of fat accumulation on VEGF expression in white adipose tissues of db/db mice. Whole tissue weights of mesenteric and subcutaneous fat were increased gradually during growth (Fig. 3*A*). Total cell counts were significantly decreased during growth only in mesenteric adipose tissues (Fig. 3*B*). A significant correlation between fat weight and VEGF expression levels was observed in mesenteric adipose tissue but not in subcutaneous adipose tissue (Fig. 4*A*). Moreover, cellular levels of VEGF expression were calculated from the results of mRNA expression levels and total cell counts in adipose tissues and positively correlated for adiposity in mesenteric adipose tissue but not in subcutaneous adipose tissue (Fig. 4*B*).

Growth-dependent change of VEGF expression in adipocytes of visceral area of db/db mice. VEGF expressions in adipocyte fraction were increased during growth (Fig. 5). Cellular expression levels of VEGF mRNA in visceral adipocytes were increased sevenfold in 18-wk-old mice compared

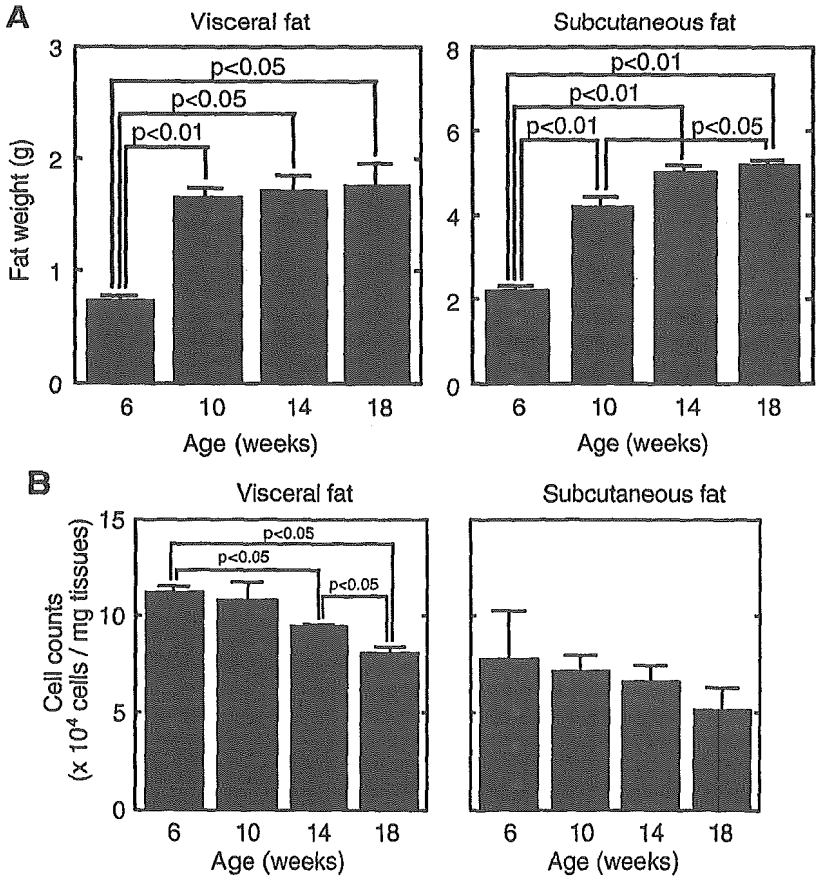

Fig. 3. Growth-dependent changes of fat weight and adiposity in mesenteric and subcutaneous adipose tissues. *A*: Time course changes of mesenteric and subcutaneous adipose tissue weights in *db/db* mice. The *db/db* mice were killed by cervical dislocation at 6, 10, 14, and 18 wk of age before adipose tissues were collected. Mesenteric and subcutaneous fat was weighed on an analytic balance. Results are represented as means + SD. *B*: Time course change of adiposity of mesenteric and subcutaneous adipose tissues in *db/db* mice. Mesenteric and subcutaneous fat was digested with collagenase S-1 and processed for cell counts using a Neubauer chamber. Results are represented as means + SD.

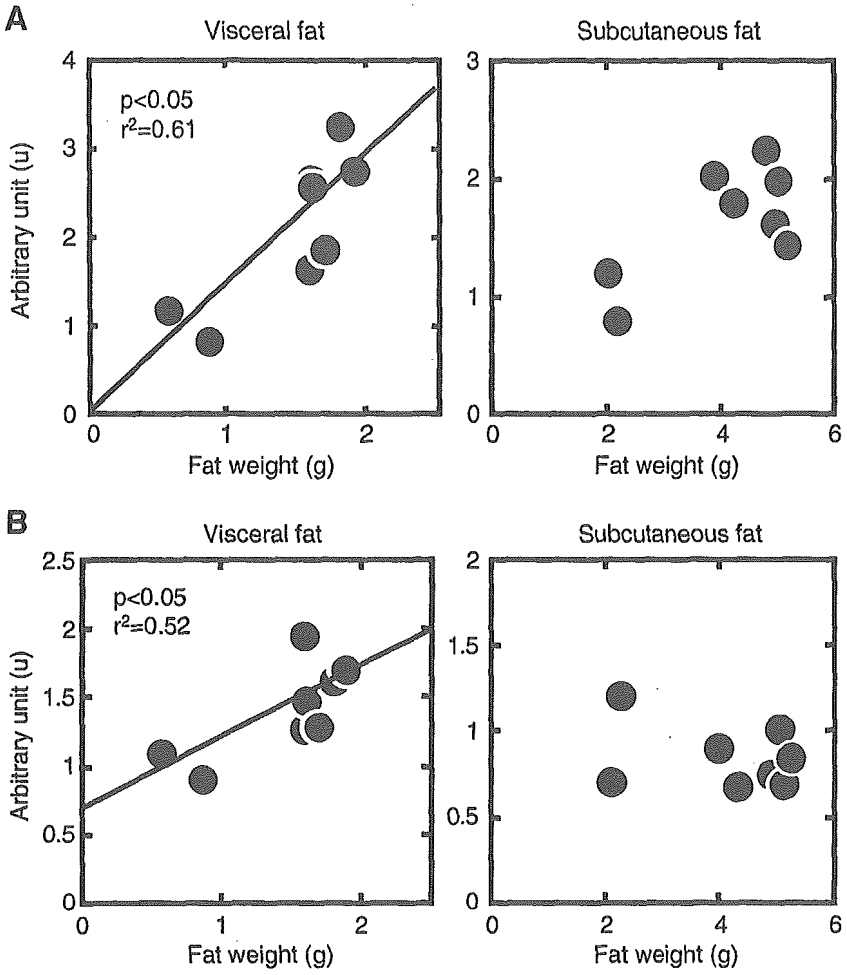

Fig. 4. Correlation between fat weight or adiposity and VEGF expressions in mesenteric adipose tissue. *A*: positive correlation between fat weight and tissue VEGF expression in mesenteric adipose tissues. *B*: positive correlation between fat weight and cellular VEGF expression in mesenteric adipose tissues.

with those in 6-wk-old mice. These results suggest that circulating VEGF concentrations in *db/db* mice were increased by the enhancement of VEGF mRNA expression in visceral adipocytes.

Plasma concentration and tissue expression of VEGF in KK-A^y mice. To demonstrate the correlation between VEGF expression and adiposity in another model of obesity, we analyzed KK-A^y mice. Plasma VEGF concentrations were significantly increased in both 8- and 16-wk-old KK-A^y mice compared with those in age-matched control mice (Fig. 6*A*). Moreover, expression levels of VEGF mRNA in visceral fat were significantly increased in KK-A^y mice compared with those in control mice (Fig. 6*B*). These results suggest that circulating VEGF concentrations in KK-A^y mice as well as in *db/db* mice were increased by the enhancement of VEGF mRNA expression in visceral fat.

Change of VEGF expressions during differentiation and maturation process in 3T3-L1 cells. We performed RT-PCR analysis for the gene expression of VEGF, PPARγ, and GLUT4 in cultured 3T3-L1 cells. VEGF mRNA was expressed even in the preadipocyte condition (Fig. 7*A*), and its expression was enhanced during adipocyte conversion. Especially, the expression levels of VEGF mRNA were significantly increased 14 days after differentiation (Fig. 7*B*). Both PPARγ and GLUT4 expressions were gradually enhanced during differentiation (Fig. 7*A*). These results suggest that expression levels of VEGF mRNA in 3T3-L1 cells were enhanced during lipid accumulation.

VEGF concentrations of conditioned media cultured with pre- and postdifferentiated 3T3-L1 cells. 3T3-L1 cells secreted VEGF proteins into culture medium even in the preadipocyte condition (Table 1), and the VEGF protein secretion was enhanced during adipocyte conversion. Especially, the VEGF concentrations in conditioned medium were increased fourfold 14 days after differentiation compared with those of predifferentiation. These results suggest that protein secretion as well as mRNA expression of VEGF in 3T3-L1 cells were enhanced during lipid accumulation. The biological activity of VEGF should be examined to know the role of VEGF in physiological and pathological conditions. Therefore, we demonstrated the angiogenic activity of conditioned medium from cultured adipocytes.

Enhancement of tube formation activity in HUVECs by addition of conditioned medium cultured with 3T3-L1 cells. VEGF secreted from both pre- and postdifferentiated 3T3-L1 cells had stimulatory activity toward HUVECs in tube formation (Fig. 8, *A* and *B*). The stimulatory activity in the condi-

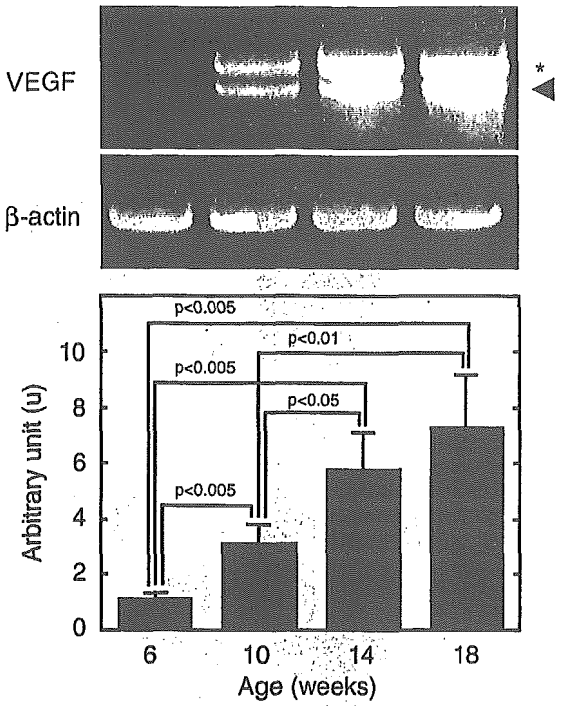

Fig. 5. Time course change of VEGF expressions in adipocyte fraction prepared from mesenteric fat of *db/db* mice. Visceral fat was cut into small pieces and digested using collagenase S-1. Then, the tissues were suspended with PBS and separated by centrifugation. The floating layer was collected as adipocyte fraction. Images show RT-PCR products of VEGF amplified from total RNA prepared from 2×10^4 cells of adipocytes at 6, 10, 14, and 18 wk after birth. The PCR products of VEGF were densitometrically analyzed, and the relative amounts at 6 wk old were set to 1.0. Results are represented as means and SD. Arrowhead, $VEGF_{164}$; *, $VEGF_{188}$.

tioned medium derived from postdifferentiated 3T3-L1 cells was three times higher than in predifferentiated cells. Moreover, anti-VEGF-neutralizing antibody apparently inhibited the stimulatory tube formation activity in both pre- and postdifferentiated 3T3-L1 cells. These findings suggest that 3T3-L1 cells secrete the bioactive form of VEGF protein.

Effect of implantation of 3T3-L1 preadipocytes into mesenteric or subcutaneous fat area of nude mice on VEGF expression. We performed RT-PCR analysis for gene expressions of VEGF, PPARγ, and GLUT4 in the mesenteric or subcutaneous fat area implanted with 3T3-L1 cells. As shown in Fig. 9*A*, the content of VEGF expression was increased fourfold in the mesenteric fat implanted with 3T3-L1 cells compared with those in sham-operated control mice. In contrast, VEGF expression of subcutaneous fat was almost the same in the mice implanted with 3T3-L1 cells into the subcutaneous area and controls. Moreover, PPARγ expression was enhanced only in mesenteric fat implanted with 3T3-L1 cells but not in subcutaneous fat. The expression levels of GLUT4 in both mesenteric and subcutaneous fat implanted with 3T3-L1 cells were higher than in controls.

The plasma VEGF concentration increased after implantation with 3T3-L1 cells into the mesenteric area, and these reached 381 ± 63 pg/ml at 4 wk. However, the mice injected in the subcutaneous area did not show any difference from control mice (Fig. 9*B*).

DISCUSSION

In the first set of experiments, we showed that the plasma VEGF concentrations gradually increased during growth in both *db/db* and *db/+* mice. After 10 wk of age, however, plasma VEGF concentrations were higher in *db/db* mice than in *db/+* mice. The *db/db* mice are considered to be an obesity model because fat deposition is the primary change. Then we analyzed the correlation between plasma VEGF concentration and body weight. The plasma VEGF concentration in *db/db*

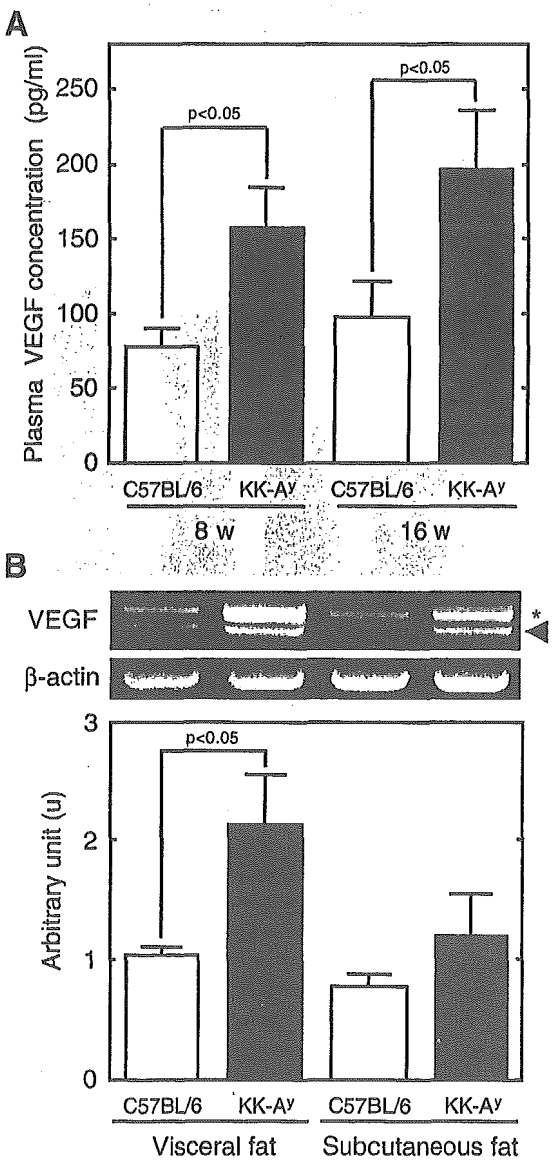

Fig. 6. Plasma concentration and tissue expression of VEGF in KK-A^y mice. *A*: comparison of plasma VEGF concentrations between KK-A^y and C57BL/6 mice. Plasma VEGF concentrations were measured in 8- and 16-wk-old KK-A^y and C57BL/6 mice. Results are represented as means + SD. *B*: comparison of VEGF gene expressions in visceral and subcutaneous adipose tissues between KK-A^y and C57BL/6 mice. Images show RT-PCR products of VEGF amplified from total RNA in mesenteric and subcutaneous adipose tissues at 16 wk after birth. The PCR products of VEGF were densitometrically analyzed, and the relative amounts in visceral adipose tissues of control mice were set to 1.0. Results are represented as means + SD. Arrowhead, $VEGF_{164}$; *, $VEGF_{188}$.

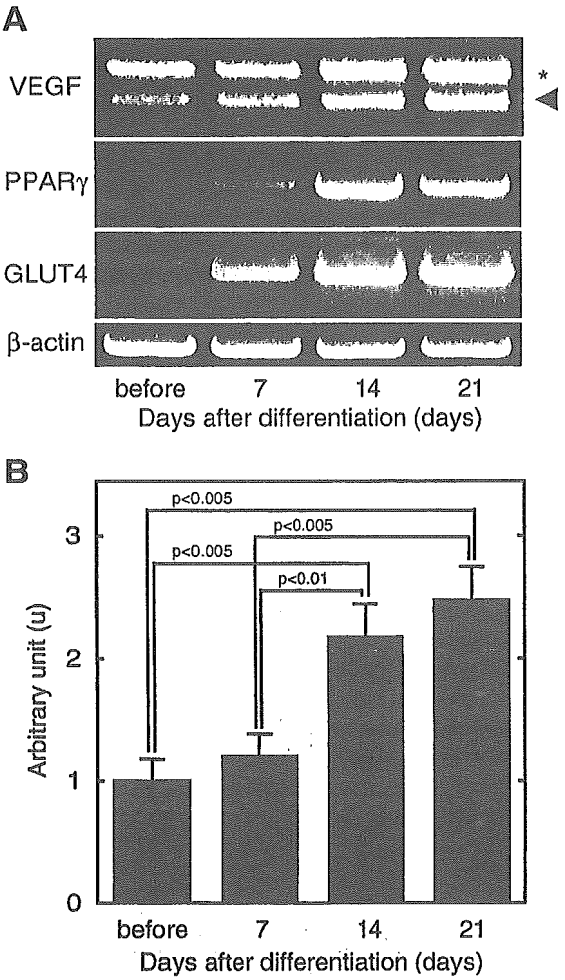

Fig. 7. Time course changes of VEGF, peroxisome proliferator-activated receptor-γ (PPARγ), and GLUT4 expressions in 3T3-L1 cells during adipocyte differentiation. *A*: gene expression profiles in 3T3-L1 cells during adipocyte differentiation. Images show RT-PCR products of VEGF, PPARγ, and GLUT4 amplified from total RNA in 3T3-L1 cells at 0, 7, 14, and 21 days after differentiation. *B*: relative amounts of VEGF expressions in 3T3-L1 cells during adipocyte differentiation. The PCR products of VEGF were densitometrically analyzed, and the relative amounts in predifferentiated 3T3-L1 cells were set to 1.0. Results are represented as means + SD. Arrowhead, $VEGF_{164}$; *, $VEGF_{188}$.

mice was significantly related to their body weight, the same as our previous results in human subjects (15). These results suggest that plasma VEGF may be determined by body fat deposition in mice.

In our previous report (15), plasma VEGF concentrations were revealed to be dependent on visceral fat accumulation. Therefore, to clarify the VEGF expressions with regard to whether subcutaneous or visceral adipose tissue affects plasma VEGF concentration in *db/db* mice, we examined mRNA expressions and protein contents of VEGF in visceral and subcutaneous adipose tissues during growth. The mRNA ex-

Table 1. *VEGF concentrations of conditioned media cultured with pre- and postdifferentiated 3T3-L1 cells*

	Days			
Differentiation periods	0	7	14	21
VEGF concentration, ng/ml	0.6±0.1	0.9±0.2	2.4±0.5	2.6±0.2
Total protein concentration, mg/ml	0.4±0.1	0.4±0.1	0.4±0.2	0.4±0.2

Values are means ± SD. VEGF, vascular endothelial growth factor.

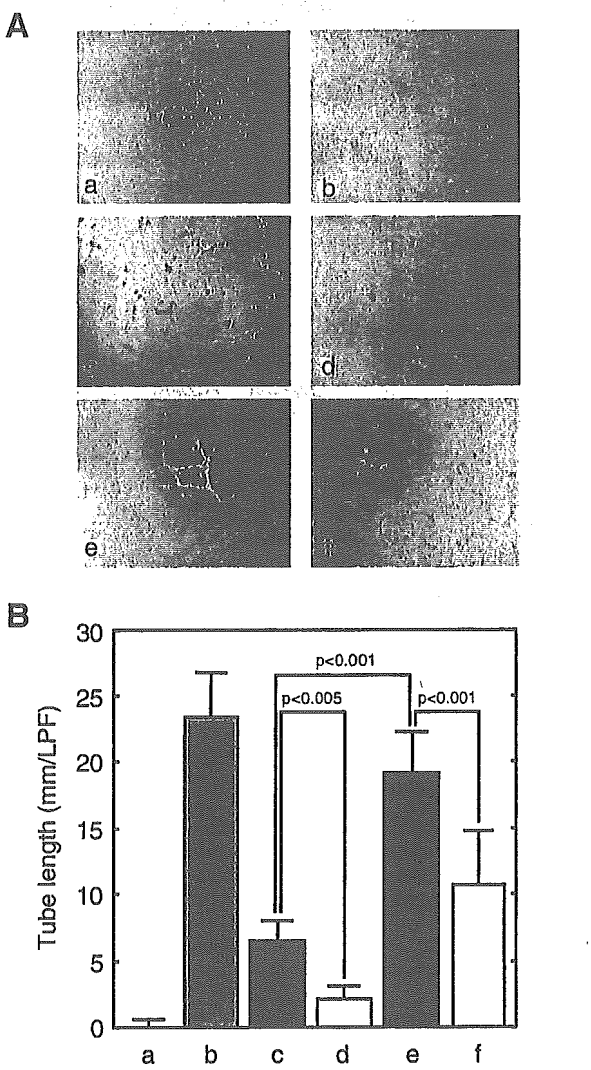

Fig. 8. Effect of conditioned media cultured with pre- and postdifferentiated 3T3-L1 cells on tube formation activity in human umbilical vein endothelial cells (HUVECs). *A*: light microscopic findings of tube formation of HUVECs in various conditions. Formation of capillary tube-like structures by HUVECs was assessed in a Matrigel-based assay as previously described (8). HUVECs were seeded on Growth Factor Reduced BD Matrigel matrix with conditioned medium derived from pre- or postdifferentiated 3T3-L1 cells in the presence or absence of anti-mouse VEGF-neutralizing antibody or recombinant VEGF protein. After 13 h of stimulation, phase-contrast microscopic low-power fields (×100) were photographed. *a*: medium alone; *b*: stimulated with recombinant VEGF (5 ng/ml); *c* and *d*: with conditioned medium from predifferentiated 3T3-L1 cells; *e* and *f*: with conditioned medium from postdifferentiated 3T3-L1 cells; *c* and *e*: in the absence of anti-VEGF antibody; *d* and *f*: in the presence of anti-VEGF antibody. *B*: tube length of HUVECs stimulated with conditioned medium prepared from pre- or postdifferentiated 3T3-L1 cells. The total length of capillary tubes formed by HUVECs in 3 different photographs per well were measured using a scale ruler. *Bar a*, medium alone; *bar b*, recombinant VEGF (5 ng/ml); *bar c*, conditioned medium from predifferentiated 3T3-L1 cells alone; *bar d*, conditioned medium from predifferentiated 3T3-L1 cells with anti-VEGF antibody; *bar e*, conditioned medium from postdifferentiated 3T3-L1 cells alone; *bar f*, conditioned medium from postdifferentiated 3T3-L1 cells with anti-VEGF antibody.

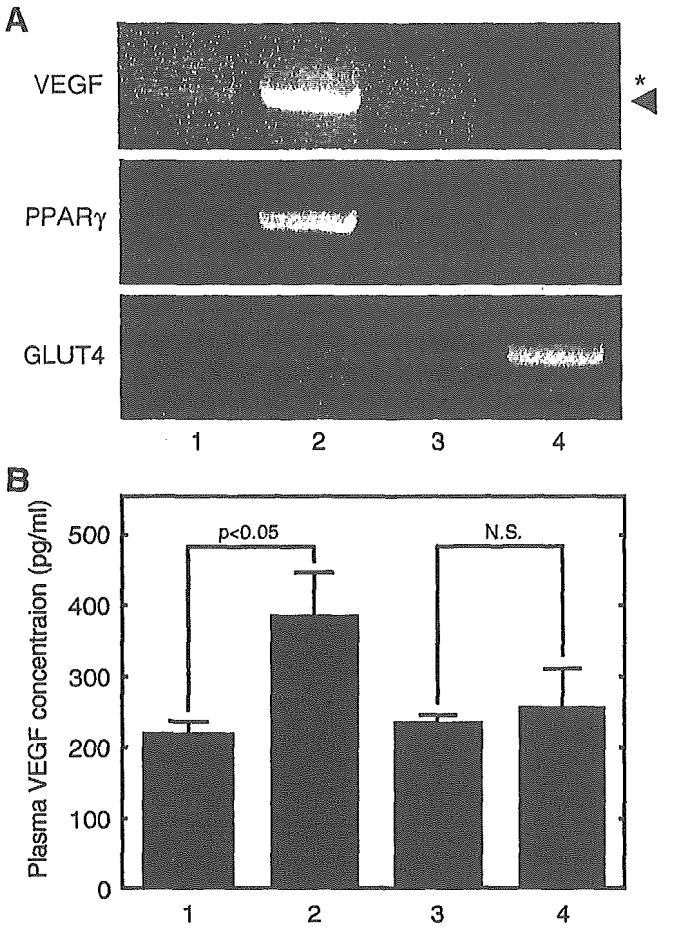

Fig. 9. Comparison of VEGF, PPARγ, and GLUT4 expressions among mice implanted with 3T3-L1 cells into mesenteric or subcutaneous fat area and controls. *A*: gene expression profiles in 3T3-L1 cells implanted into adipose tissues of nude mice. Images show RT-PCR products of VEGF, PPARγ, and GLUT4 amplified from total RNA in adipose tissues. *Lane 1*, mesenteric adipose tissues injected with PBS alone; *lane 2*, mesenteric adipose tissues injected with 3T3-L1 cells; *lane 3*, subcutaneous adipose tissues injected with PBS alone; *lane 4*, subcutaneous adipose tissues injected with 3T3-L1 cells. Arrowhead, $VEGF_{164}$; *, $VEGF_{188}$. *B*: plasma VEGF concentrations in mice implanted with 3T3-L1 cells. Plasma VEGF concentrations were measured at 4 wk after implantation with 3T3-L1 cells. *Lane 1*, mice injected with PBS alone into mesenteric area; *lane 2*, mice injected with 3T3-L1 cells into mesenteric area; *lane 3*, mice injected with PBS alone into subcutaneous area; *lane 4*, mice injected with 3T3-L1 cells into subcutaneous area.

pression levels of VEGF in visceral fat were more enhanced than in subcutaneous fat. Furthermore, the protein contents were enhanced in visceral fat but not in subcutaneous fat. These results suggest that plasma VEGF concentrations are revealed to be dependent on visceral fat accumulation even in mice.

The expression levels of TNF-α and PAI-1 in adipocytes are reported to be directly related to the degree of differentiation from preadipocytes and to be dependent on their anatomic location (12, 14, 20, 21). Therefore, we demonstrated the degree of fat accumulation in adipocytes and the correlation between VEGF mRNA expressions and adiposity in subcutaneous and mesenteric adipose tissues. Whole tissue weights of mesenteric and subcutaneous fat were increased gradually during growth. However, total cell counts were significantly decreased during growth in mesenteric fat but not in subcutaneous fat. A significant correlation between VEGF mRNA expressions and weight and adiposity in mesenteric adipose tissue was observed, but not in subcutaneous adipose tissue. These results suggest that the increase of weight in mesenteric adipose tissue is dependent on fat accumulation in adipocytes but not in subcutaneous adipose tissue. Moreover, VEGF expression is dependent on the levels of fat deposition in adipocytes. Then, we isolated the adipocyte fraction from mesenteric fat and examined VEGF mRNA expression in adipocytes. VEGF expression levels in the adipocyte fraction were also increased during growth.

Next, we examined the relation between VEGF expression and degree of differentiation using 3T3-L1 cells, an established adipocyte cell line. VEGF mRNA was expressed even in the preadipocyte condition, and its expression was enhanced after adipocyte conversion. Especially, the expression levels of VEGF mRNA were significantly increased 14 days after differentiation. Furthermore, the levels of VEGF protein secretion were almost the same level as gene expression. These results suggest that VEGF production may be dependent on the lipid accumulation (maturation) as well as the time lapse after adipocyte conversion rather than adipocyte differentiation from preadipocytes in 3T3-L1 cells.

We next determined whether VEGF protein secreted from 3T3-L1 cells has some biological activities. To know the role of VEGF in physiological or pathological conditions, we examined the effect of conditioned medium derived from 3T3-L1 cells on in vitro tube formation activity in HUVECs. The conditioned media from pre- and postdifferentiated 3T3-L1 cells enhanced angiogenesis in vascular endothelial cells. These results suggest that VEGF protein secreted from adipocytes may play some roles in the pathological neovascularization observed in diabetic retinopathy or atherosclerosis.

In the third set of experiments, the effects of anatomic localization on fat accumulation and VEGF production in adipocytes were analyzed using a cell implantation technique. 3T3-L1 cells implanted into the mesenteric area of athymic mice expressed more VEGF mRNA than that implanted into the subcutaneous area. The expression of PPARγ was also higher in 3T3-L1 cells implanted into the mesenteric area than into the subcutaneous area, and plasma VEGF concentrations in the mice implanted with 3T3-L1 cells into the mesenteric area were higher than in the subcutaneous area. These results suggest that a certain mechanism may exist in the visceral fat area to make implanted 3T3-L1 cells for enhanced VEGF production.

In summary, these results from in vitro and in vivo experiments indicate that VEGF expression in adipocytes is possibly differentiation as well as time (age) dependent after adipocyte conversion and may be determined by the site of body distribution. Further experiments are required to clarify the mechanism of enhanced expression of VEGF in visceral fat.

GRANTS

These studies were supported by grants from the Japanese Ministry of Education, Science, Sports and Culture.